Lap Splices in Unconfined Boundary Elements

Tests indicate that a currently allowed detail provides insufficient toughness

by John N. Hardisty, Enrique Villalobos, Brian P. Richter, and Santiago Pujol

Because lap splices are believed to limit frame toughness, they are not used near critical sections of frames that are required to resist earthquake demands. Nevertheless, the current building code[1] still allows lap splices at the bases of structural walls, where large inelastic deformations are expected to take place during strong ground motions. In the most critical cases, these splices are not located within confined boundary elements.

Certainly, the tensile strength of lap splices has been studied extensively.[2] However, failures of unconfined deformed-bar lap splices observed after recent seismic events in Turkey,[3] Japan,[4] and Chile[5] indicate a need to revisit the topic.

In buildings with structural walls, wall toughness is critical to seismic response. While most structural walls are currently constructed with lap splices at their bases, information on the deformation capacity of such walls is scarce.[6,7] The work described herein was aimed at generating data to help fill that gap.

Experimental Program

Six beams and two structural walls were tested. For the beams, test variables included the type of hook on the transverse reinforcement, spacing of the longitudinal and transverse reinforcement, and whether the reinforcing steel had a well-defined yield plateau. For the walls, test variables included the type of hook on the transverse reinforcement and the spacing of the longitudinal reinforcement. This article comprises a summary of the work. Detailed information can be accessed at **http://nees.org/warehouse/project/1130** and **http://nees.org/warehouse/project/1050**. Beams T-60-8-A, B, and C were tested by Richter.[8] Walls were tested by Villalobos.[9] Beams T-60-8-D, E, and F are not reported anywhere else.

Beams

Table 1 summarizes specimen properties for the test beams. Test beams (Fig. 1) were designed with stems (webs) proportioned to replicate the boundary elements of relatively thin structural walls. Longitudinal tension reinforcement comprised four No. 8 bars located in the web (Fig. 1(a)). The clear cover to the transverse reinforcement was 3/4 in. (19 mm), which is typical in structural walls today. The minimum clear cover over the longitudinal bars was 1-1/8 bar diameters. The effective depth d, the distance between extreme compression fiber and the centroid of longitudinal reinforcement, was 25-7/8 in. (657 mm) for all beams except Beam T-60-8-B, which had a d of 26-3/8 in. (670 mm). Beam T-60-80-B was designed to mimic structural walls constructed in Chile, with close longitudinal bar clear spacing s_c in lap splices in wall boundary elements.[5]

Longitudinal reinforcement ratios ρ were 0.63% and 0.61% outside the spliced region and 1.26% and 1.22% inside the spliced region. Stirrup types, center-to-center spacing s, and the resulting transverse reinforcement ratios ρ_v are provided in Table 1 and Fig. 2 (note that Beam T-60-8-C had no transverse reinforcement).

The beams were cast with the No. 8 longitudinal bars at the bottom of the formwork to avoid top-casting effects. Before testing, the beams were rotated 180 degrees about the longitudinal axis so that the longitudinal bars were at the top of the beam during testing.

Walls

Two wall specimens, W-60-N and W-60-N2, were tested. Each specimen consisted of a footing and a wall (Fig. 3). The footing was fastened to the laboratory floor, and lateral load was applied near the top of the wall. Each footing was 8 ft (2.44 m) long, 4 ft (1.22 m) wide, and 3 ft (0.91 m) thick. Each wall was centered on its footing and was 8 in. (203 mm) thick (b_w), 5 ft (1.52 m) long (L_w), and 12 ft (3.66 m) tall.

Details of the reinforcement layout and dimensions for the walls are shown in Fig. 4. Longitudinal reinforcement comprised four No. 8 bars in each boundary element (providing tension reinforcement A_s of 3.16 in.^{2} [2039 mm^2]) and six No. 4 bars distributed in two layers in the web and spaced at 12 in. (305 mm) on center. The longitudinal bars were lap

Table 1:
Summary of properties for beam test specimens

Beam label	Clear spacing between spliced bars s_c	Stirrup type*	Center-to-center spacing of transverse reinforcement s, in. (mm)	Transverse reinforcement ratio ρ_v, %	Well-defined yield plateau	Yield stress f_y, ksi (MPa)		Compressive strength f_c', psi (MPa)
						No. 8 bars†	No. 3 bars‡	
T-60-8-A	1.5 d_b	II	5 (127)	0.55	Y	65 (448)	63 (434)	4300 (29.6)
T-60-8-B	0.5 d_b	I	5 (127)	0.55	Y	66 (455)	63 (434)	4100 (28.3)
T-60-8-C	1.5 d_b	—	—	0.0	Y	66 (455)	63 (434)	4100 (38.3)
T-60-8-D	1.5 d_b	III	8 (203)	0.34	N	63§ (434)	63 (434)	5900 (40.7)
T-60-8-E	1.5 d_b	I	8 (203)	0.34	N	63§ (434)	63 (434)	5200 (35.9)
T-60-8-F	1.5 d_b	III	11 (279)	0.25	N	63§ (434)	63 (434)	6300 (43.4)

*Refer to Fig. 2

†Boundary-element longitudinal bars

‡Bars used for stirrups

§Taken as f_s at 0.2% offset

Note: d_b is longitudinal bar diameter

spliced at the base of the walls, with splice lengths of 60 bar diameters. The minimum clear cover to the longitudinal bars was 1.1 bar diameters. Table 2 lists the main properties of the walls. For both walls, the effective depth to the boundary-element longitudinal bars was approximately 4 ft 8 in. (1.42 m).

Transverse reinforcement in both walls consisted of two No. 3 ties spaced at 5 in. (127 mm) on center, resulting in a transverse reinforcement ratio of 0.55%. The clear cover to the transverse reinforcement was 3/4 in. (19 mm). Wall W-60-N had ties similar to the Type II stirrups of Beam T-60-8-A, while Wall W-60-N2 had ties similar to the Type I stirrups of Beam T-60-8-B (refer to Fig. 2 and Fig. 4).

The wall specimens were cast vertically in three lifts—one for the footing and two for the wall. The resulting cold joints were cleaned, roughened, and moistened before casting the subsequent lift.

Test Setup, Instrumentation, and Procedure

Beams

The beam test setup is shown in Fig. 1(b). The beams were loaded in four-point bending with their webs in tension. Lap splices, all with lap lengths of 60 bar diameters, were located in the constant moment region between the supports. Load was applied by four 30 ton (300 kN) center-hole hydraulic

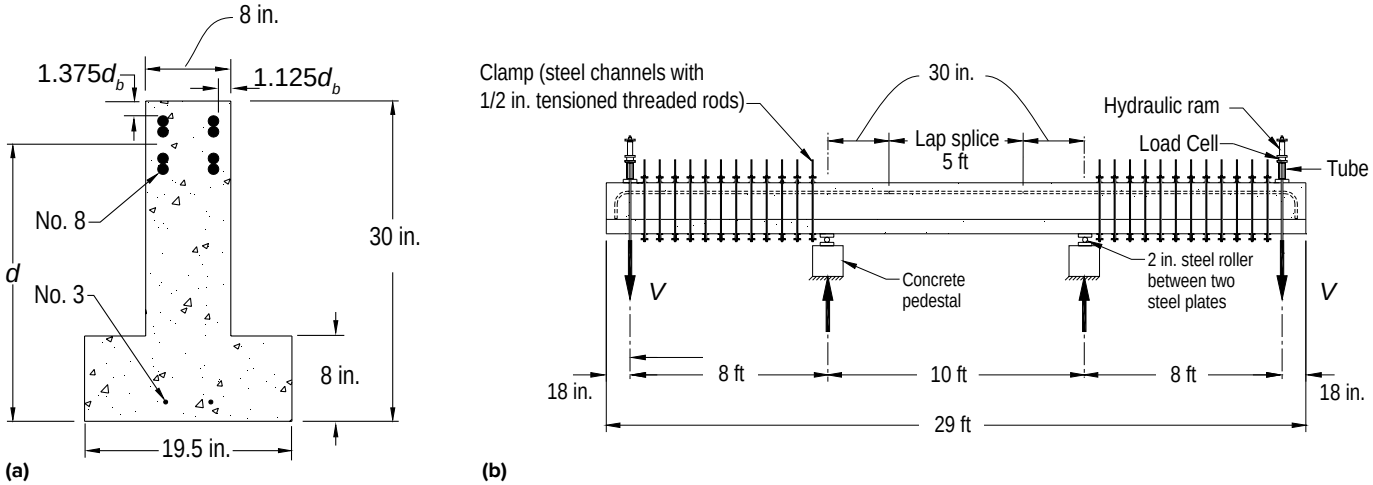

Fig. 1: Geometry of test beams: (a) section; and (b) elevation and test setup (Note: 1 in. = 25.4 mm; 1 ft = 0.3 m)

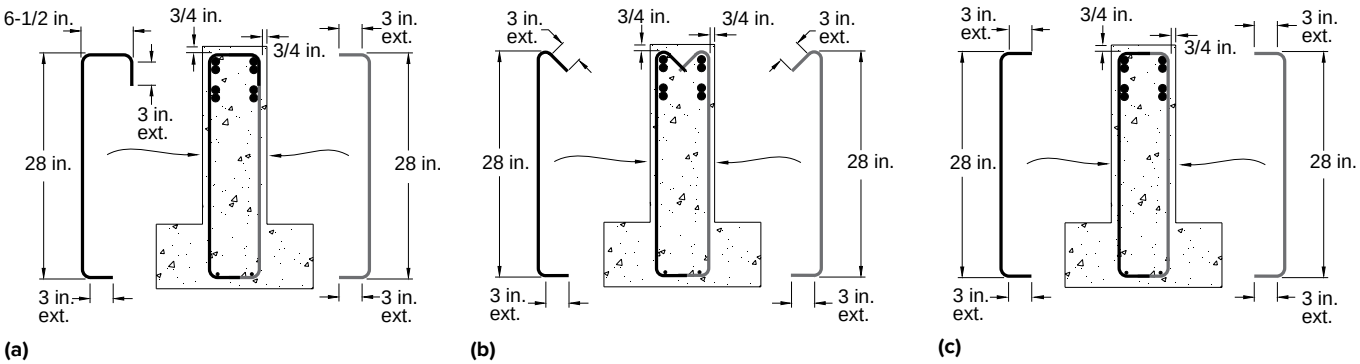

Fig. 2: Stirrup types: (a) Type I, used in Beams T-60-8-B and E; (b) Type II, used in Beam T-60-8-A; and (c) Type III, used in Beams T-60-8-D and F (Note: 1 in. = 25.4 mm; stirrup types shown for Beams T-60-8-A and B (in Fig. 2-7 and 2-8) in Reference 8 were accidentally interchanged). All stirrups were fabricated using No. 3 bars

Table 2:
Summary of properties for wall test specimens

Wall label	Clear spacing between spliced bars s_c	Tie type*	Yield stress f_y, ksi (MPa)			Compressive strength f_c', psi (MPa)
			No. 8 bars†	No. 4 bars‡	No. 3 bars§	
W-60-N	$1.75d_b$	II	67 (462)	63 (434)	77 (531)	4300 to 4900 (39.6 to 33.8)
W-60-N2	$0.5d_b$	I	68 (469)	63 (434)	66 (455)	4600 to 4700 (31.7 to 32.4)

*Refer to Fig. 4

†Boundary-element longitudinal bars

‡Web longitudinal bars

§Bars used for ties

Note: d_b is longitudinal bar diameter

rams (two rams at each load point) that reacted against high-strength threaded rods anchored to the laboratory strong floor.

During testing, load was increased monotonically until the longitudinal reinforcement yielded or the specimen failed (whichever occurred first). Loading was increased at 8 kip (35.6 kN) increments (at each end). If yield was reached, loading was stopped and the specimen was unloaded. The specimen was reloaded to the same load seven times (Beams T-60-8-A and B) or 10 times (Beams T-60-8-D, E, and F). Beam T-60-8-C failed before yield. If failure did not take place in the reloading at the yield force, the load was increased to reach a displacement equal to twice the displacement at first yield. This procedure was repeated until failure. Load and vertical displacements were monitored continuously throughout the test. Vertical displacement was measured at the load points, midspan, and splice ends. Figures 5 and 6 provide examples of measured load-deflection curves.

Walls

The wall test setup is shown in Fig. 3. Eight post-tensioning bars (four 1-3/8 in. [35 mm] diameter bars at the corners of the footing and four 1-1/4-in. [32 mm] diameter bars near the center of the footing) fastened the footing to the laboratory reaction floor with a total force of 960 kip (4270 kN). The north and south faces of the footing were butted against steel reaction blocks to prevent slip. Each reaction block was post-tensioned to the laboratory floor with a force of 600 kip (2670 kN).

An axial load of 200 kip (890 kN) was applied at the top of each wall by four 1-1/4 in. (32 mm) in diameter post-tensioning bars tensioned by hydraulic rams reacting on steel tubes that rested on top of the wall. The rams were connected to a manifold and were continuously controlled by a single manual pump during the tests to maintain the axial load within 1% of the target load (±2 kip [8.9 kN]).

Lateral load was applied by two hydraulic actuators with swivels at both ends and attached to the test walls through load tubes perpendicular to the in-plane direction of the wall on either side. The load rig was attached to the wall by two, 1-1/4 in. (32 mm) in diameter, post-tensioning bars reacting on either tube and tensioned by hydraulic rams. The distance from the top of the footing to the point of load application (that is, the clear wall height) was 10 ft, 10-1/2 in. (3.32 m). Lateral bracing was provided by square

steel tubes on either side of the wall at 10 ft (3.05 m) from the top of the footing.

The test procedure consisted of slowly applied displacement reversals, increasing in magnitude up to failure. Three cycles were applied at each of the following target drift ratios: 1/8, 1/4, 1/2, 3/4, 1, 1-1/2, 2, 2-1/2, and 3% of the clear wall height.

The applied lateral load, axial load, and displacements of the footing and along the height of the wall were measured continuously throughout the test.

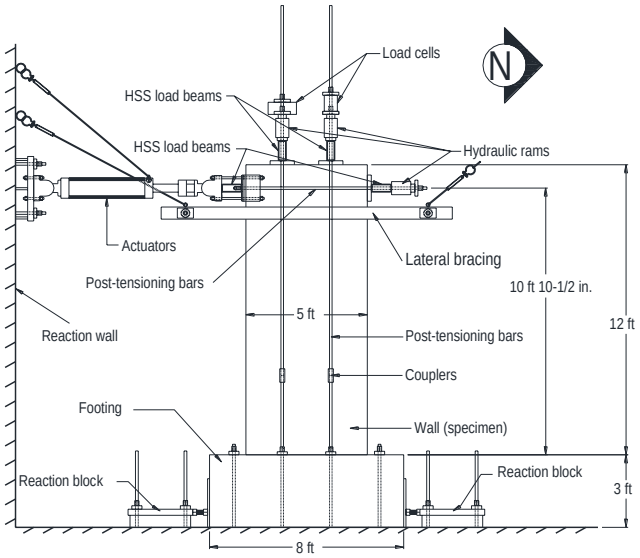

Fig. 3: Test wall east elevation and setup (Note: 1 ft = 0.3 m)

Material Properties

Concrete compressive strength was obtained from compression tests of 6 x 12 in. (152 x 305 mm) cylinders. Stress-strain relationships for the reinforcing steel were obtained from standard tensile tests. Three coupons from each heat of steel were tested.

Beams

For the beams, concrete compressive strength at the time of testing ranged from 4100 to 6300 psi (28.3 to 43.4 MPa). The reinforcing bars were certified as meeting ASTM A615/A615M, "Standard Specification for Deformed and Plain Carbon-Steel Bars for Concrete Reinforcement." Our tests showed, however, that the bars met the tensile yield stress requirement described in ASTM A706/A706M, "Standard Specification for Deformed and Plain Low-Alloy Steel Bars for Concrete Reinforcement."

For Beams T-60-8-A, B, and C, the longitudinal steel had a well-defined yield plateau. For Beams T-60-8-D, E, and F, the longitudinal reinforcing steel did not have a well-defined yield plateau. In all beams, the yield stress of the transverse reinforcement was 63 ksi (434 MPa). Material properties for each beam are listed in Table 1.

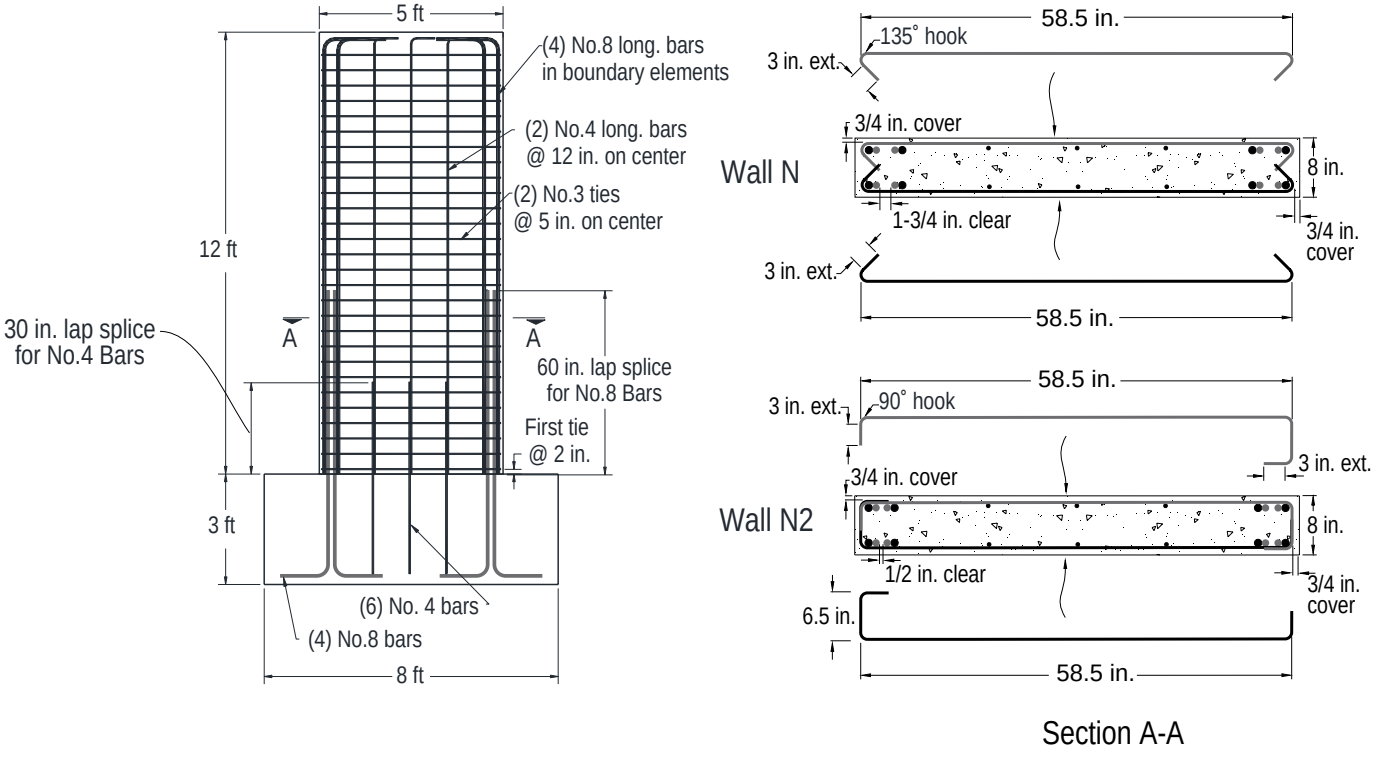

Fig. 4: Wall reinforcement layout and dimensions (Note: 1 in. = 25.4 mm; 1 ft = 0.3 m)

Table 3:
Summary of test results for beam test specimens

Beam label	Peak load reached during reloading, kip (kN)			Maximum applied load V_u, kip (kN)	Midspan deflection at maximum applied load Δ_u, in. (mm)	Midspan deflection at yield Δ_y, in. (mm)	Δ_u/Δ_y	Δ_u/L_{CL}, %	Δ_y/L_{CL}, %
	V_1	V_2	V_3						
T-60-8-A	55.0 (244.7)	57.0 (253.5)	59.0 (262.4)	59.4 (264.2)	0.78 (19.8)	0.20 (5.1)	3.9	1.30	0.33
T-60-8-B	56.5 (251.3)	—	—	56.7 (252.2)	0.33 (8.4)	0.21 (5.3)	1.6	0.55	0.35
T-60-8-C*	—	—	—	42.2 (187.7)	0.17 (4.3)	—	—	0.28	—
T-60-8-D	56.0 (249.1)	65.0 (289.1)	—	64.8 (288.2)	0.58 (14.7)	0.26 (6.6)	2.2	0.97	0.43
T-60-8-E	58.0 (258.0)	66.0 (293.6)	—	66.1 (294.0)	0.62 (15.7)	0.28 (7.1)	2.2	1.03	0.47
T-60-8-F	58.0 (258.0)	65.0 (289.1)	—	64.8 (288.2)	0.56 (14.2)	0.29 (7.4)	1.9	0.93	0.48

*Specimen did not reach yield

Note: L_{CL} is distance from support to centerline of beam span

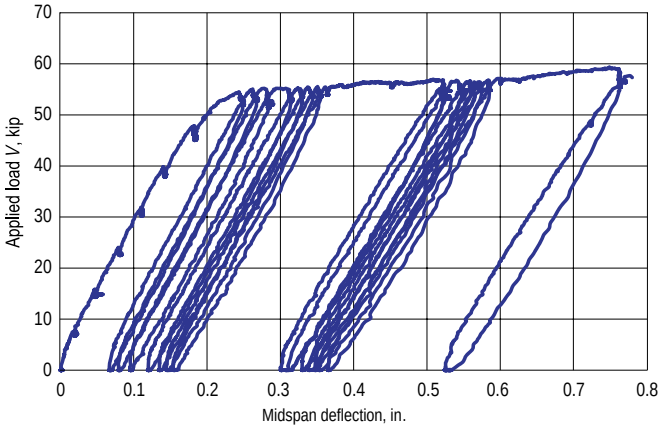

Fig. 5: Applied load *V* versus midspan deflection for Beam T-60-8-A (Note: 1 kip = 4.45 kN; 1 in. = 25.4 mm)

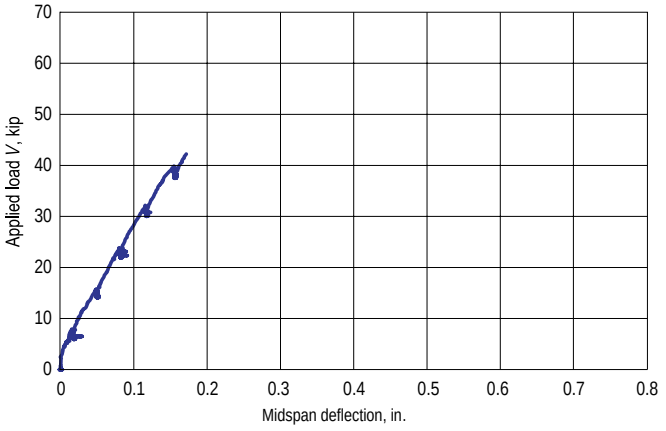

Fig. 6: Applied load *V* versus midspan deflection for Beam T-60-8-C with visible failure before yield (Note: 1 kip = 4.45 kN; 1 in. = 25.4 mm)

Walls

For the walls, the compressive strength of concrete at the time of testing ranged from 4300 to 4900 psi (29.6 to 33.8 MPa) for Wall W-60-N and from 4600 to 4700 psi (31.7 to 32.4 MPa) for Wall W-60-N2. The No. 4 longitudinal bars in both wall specimens had a yield stress of 63 ksi (434 MPa) and the No. 3 ties had a yield stress of 77 ksi (531 MPa) in Wall W-60-N and 66 ksi (455 MPa) in Wall W-60-N2. The reinforcing bars were certified as ASTM A706/A706M Grade 60. Material properties for each wall are listed in Table 2.

Test Results and Data Analyses

Table 3 provides a summary of the beam test results. Sample load-deflection curves for two specimens are presented in Fig. 5 and 6. The loads reported are the means of the loads applied at each beam end. The reported midspan deflection at yield is the midspan deflection corresponding to the intersection of a tangent to the applied load versus midspan deflection curve in the linear range of response after cracking, and a tangent to the same curve in the inelastic range of response.

Table 4 shows the measured lateral loads and drift ratios. Based on a definition of limiting drift ratio as the maximum drift ratio at which the lateral load was at least 80% of the maximum load (in each direction), the limiting drift ratio was 2% for Wall W-60-N and 1.5% for Wall W-60-N2.

Failure mechanisms

In spite of their similar tension reinforcement layouts, the wall specimens were observed to fail in compression while the beam specimens failed in bond along the splices (Fig. 7). The moment gradient over the splice length appears to have been be a major factor. While the lap splices in the walls were

Table 4:
Summary of results of wall test specimens

Wall label	Loading direction	Maximum applied load V_u, kip (kN)	Δ_u/L, %	Applied load at limiting drift ratio V_Δ, kip (kN)	Δ_Δ/L, %
W-60-N	North	159 (707)	1.5	143 (636)	2.0
	South	−155 (−689)	−1.5	−127 (−565)	−2.0
W-60-N2	North	170 (756)	1.5	142 (632)	2.0
	South	−167 (−743)	−1.5	−167 (−743)	−1.5

Note: Δ_u is deflection at maximum applied load, L is distance from top of footing to point of load application (10 ft 10-1/2 in. [3.32 m]), and Δ_Δ is limiting drift

Fig. 7: Splice failure in test beam

subjected to large moment gradients, the lap splices in the beams were subjected to a nearly constant moment over their lengths. The moment imposed on the test walls varied from zero, at the point of load application, to a maximum at the base of the wall. The moment arm for this load was 130.5 in. (3315 mm), while the length of the lap splice was 60 in. (1525 mm). The moment developed along the lap splices therefore varied from 100% of maximum at base of the wall to approximately 54% of maximum at the opposite end of the splice. In contrast, four-point bending of the test beams placed the splices in the beams in nearly constant moment.

In a multi-story building with splices at the base, the moment that would be developed in the splices would not vary much along the splice length. These observations suggest that test results for scaled structural walls with large-scale lap splices cannot be reliably projected to full-scale walls. The results from beam tests could be expected *to better represent* the performance of full-scale structural walls.

From tests of cantilever beams with the same length but different lap splice lengths, Ferguson and Briceno[10] inferred that splice strength is sensitive to the difference between the bar stresses at each end of the splice. It follows that splice strength is sensitive to moment gradient. The tests reported herein confirm this inference.

Splice strength

Table 5 shows the maximum total moments, peak steel stresses, and mean unit bond strengths computed for each layer of reinforcement. The maximum total moments and steel stresses were computed at the ends of each splice. Maximum total moment results from the maximum applied load, the weight of the test hardware, and the self-weight of each beam. The steel stresses in each reinforcement layer (maximum and at each load increment) were computed using the method outlined by Richter.[8] The data in Tables 3 and 5 show that the presence of transverse reinforcement resulted in increases in mean unit bond strength and deformation capacity.

Figure 8 shows drift ratio at failure versus transverse reinforcement ratio. The most striking feature of this plot is the magnitude of the drift ratios reached. No beam specimen went beyond a drift ratio of 1.3%. If we consider that 1) no load reversals were applied; and 2) in a strong earthquake, cover spalling is likely to occur at wall bases—where lap splices are often located—the measured drifts suggest that structural walls with details similar to those tested do not have the toughness required to survive earthquake demands.

Figure 8 also shows that at the same transverse reinforcement ratio, decreasing the clear spacing between spliced bars lowered the drift capacity at failure. This is evident in beams T-60-8-A and B.

At the same clear vertical bar spacing and hook configuration, increasing the transverse reinforcement ratio led to an increase in drift capacity. Provided that the transverse reinforcement ratio stayed the same and that minimum hook dimensions were met, transverse reinforcement detailing (hook configuration) appears to have had no appreciable effect on peak drift ratio.

In Fig. 9, it can be seen that peak reinforcement stress varied

Table 5:

Estimated maximum steel stress and mean bond stress in test beams

Beam label	Maximum total moment at slice end M_u, kip-ft (kNm)	Steel layer	Maximum steel stress at splice end f_{su}, ksi (MPa)		Mean unit bond strength μ_u, psi (MPa)		Transverse reinforcement ratio ρ_v, %
T-60-8-A	506 (686)	Top Bottom	81 (559) 80 (552)	$1235\sqrt{f_c'}$ $1220\sqrt{f_c'}$	338 (2.33) 333 (2.30)	$5.1\sqrt{f_c'}$ $5.1\sqrt{f_c'}$	0.55
T-60-8-B	485 (658)	Top Bottom	78 (538) 78 (538)	$1218\sqrt{f_c'}$ $1218\sqrt{f_c'}$	325 (2.24) 325 (2.24)	$5.1\sqrt{f_c'}$ $5.1\sqrt{f_c'}$	0.55
T-60-8-C	369 (500)	Top Bottom	65 (448) 54 (372)	$1015\sqrt{f_c'}$ $843\sqrt{f_c'}$	271 (1.87) 225 (1.55)	$4.2\sqrt{f_c'}$ $3.5\sqrt{f_c'}$	0.00
T-60-8-D	550 (746)	Top Bottom	86 (593) 84 (579)	$1120\sqrt{f_c'}$ $1094\sqrt{f_c'}$	358 (2.47) 350 (2.41)	$4.7\sqrt{f_c'}$ $4.6\sqrt{f_c'}$	0.34
T-60-8-E	560 (759)	Top Bottom	88 (607) 86 (593)	$1220\sqrt{f_c'}$ $1193\sqrt{f_c'}$	367 (2.53) 358 (2.47	$5.1\sqrt{f_c'}$ $5.0\sqrt{f_c'}$	0.34
T-60-8-F	550 (746)	Top Bottom	86 (593) 84 (579)	$1083\sqrt{f_c'}$ $1058\sqrt{f_c'}$	358 (2.47) 350 (2.41)	$4.5\sqrt{f_c'}$ $4.4\sqrt{f_c'}$	0.25

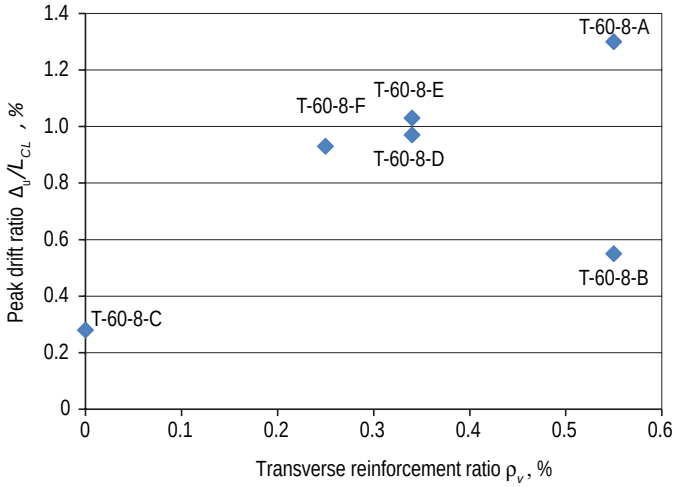

Fig. 8: Peak drift ratio versus transverse reinforcement ratio for test beams

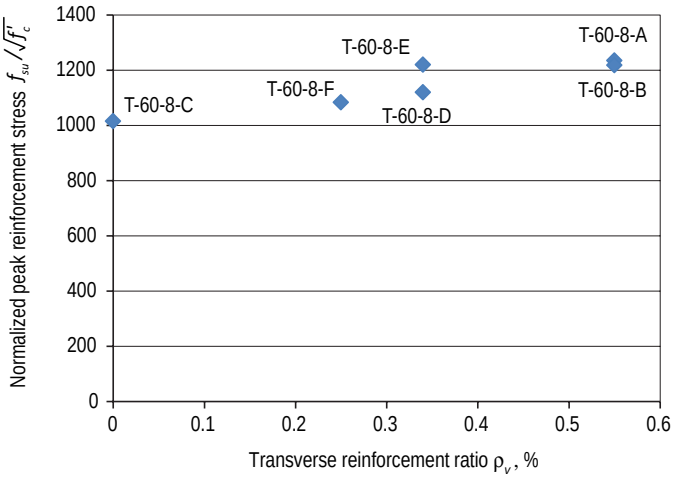

Fig. 9: Peak mean reinforcement stress versus transverse reinforcement ratio for test beams

linearly with transverse reinforcement ratio. While vertical bar clear spacing and transverse reinforcement detailing appear to have had little effect on maximum stress, variations in bar clear spacing did appear to affect drift ratios at failure (Fig. 8).

Summary and Conclusions

Tests were conducted on six test beams and two scaled walls that were designed to represent 8 in. (200 mm) thick structural walls with lap splices in unconfined boundary elements. The subject is relevant because unconfined lap splices at bases of structural walls are allowed by the current building code. The test beams were evaluated in constant moment, with the lap splices in tension. Lap splice length was $60d_b$ and met current design requirements, while concrete strength and transverse reinforcement ratio varied from approximately 4100 to 6300 psi (28.3 to 43.4 MPa) and 0 to 0.55%, respectively. Lap splices in all test beams failed at drift ratios ranging from approximately 0.3 to 1.3%. Boundary reinforcement in the two test walls was similar to the tensile reinforcement in the test beams. The walls were loaded as cantilevers with a horizontal in-plane load near the free end and subjected to displacement reversals. Lap splices in walls did not fail. Nevertheless, the test walls also failed at modest drift ratios (as low as 1.5%).

The most salient conclusions from the data obtained in our tests are:

- The beam test results were not affected by the shape of the stress-strain curve (the presence or absence of a well-defined yield plateau) in the longitudinal bars, suggesting that bar stress is a more critical factor affecting splices than bar strain;
- Comparisons of the responses of the beam and wall tests confirm that the strength of a lap splice is sensitive to the moment gradient over the length of the splice. Because the bases of most structural walls will be subjected to moments with small gradients, results from tests of lap splices in scaled walls cannot be projected directly to full-scale walls. A more conservative approach is to base performance projections on results from tests in which lap splices are subject to constant moment over the splice length;
- Drift capacity was modest (no more than 1% in five out of six beam tests) in beam specimens with unconfined splices. While peak bar stress and drift capacity increased with increases in transverse reinforcement ratio, these increases were offset almost completely by reductions in the clear spacing between spliced bars, which can occur easily during construction; and
- Because factors such as spalling and displacement reversals are bound to reduce further the drift capacity of walls, the observed drift capacities suggest that structural walls with unconfined lap splices at their bases do not have the toughness required to survive the demands associated with strong ground motion caused by earthquakes.

Acknowledgments

The authors would like to thank Sumo and Guito, and acknowledge the generous support of ERICO Inc. The reported tests were conducted at Bowen Laboratory, Purdue University.

References

1. ACI Committee 318, "Building Code Requirements for Structural Concrete (ACI 318-11) and Commentary," American Concrete Institute, Farmington Hills, MI, 2011, 503 pp.

2. ACI Committee 408, "Bond and Development of Straight Reinforcing Bars in Tension (ACI 408-R03)," American Concrete Institute, Farmington Hills, MI, 2003, 49 pp.

3. Kilic, S., and Sozen, M.A., "Evaluation of Effect of August 17, 1999, Marmara Earthquake on Two Tall Reinforced Concrete Chimneys," *ACI Structural Journal*, V. 100, No. 3, May-June 2003, pp. 357-364.

4. Kim, S., and Shiohara, H., "Dynamic Response Analysis of a Tall RC Chimney Damaged during 2007 Niigata-ken Chuetsu-Oki Earthquake," Paper No. 3433, *Proceedings of the Fifteenth World Conference on Earthquake Engineering*, 2012, 9 pp.

5. Song, C.; Pujol, S.; and Lepage A., "The Collapse of the Alta Rio Building during the 27 February 2010 Maule, Chile, Earthquake," *Earthquake Spectra*, V. 28, No. S1, 2012, pp. S301-S334.

6. French, C.; Lopez, R.; and Sritharan, "NEES Project Warehouse," 2005, http://nees.org/warehouse/project/22. (last accessed Mar. 3, 2014)

7. Lowes, L.; Kuchma, D.; Lehman, D.; and Zhang, J., "NEES Project Warehouse," 2004, http://nees.org/warehouse/project/104. (last accessed Mar. 3, 2014)

8. Richter, B.P., "A New Perspective on the Tensile Strength of Lap Splices in Reinforced Concrete Members," M.S. thesis, Purdue University, West Lafayette, IN, 2012, 165 pp.

9. Villalobos, E.J., "Seismic Response of Structural Walls with Reinforcement and Geometric Discontinuities," PhD thesis, Purdue University, West Lafayette, IN, 2014, 334 pp.

10. Ferguson, P. M., and Briceno, A., "Tensile Lap Splices-Part 1: Retaining Wall Type, Varying Moment Zone," Research Report No. 113-2, Center for Highway Research, The University of Texas at Austin, Austin, TX, 1969, 39 pp.

Note: Additional information on the ASTM standards discussed in this article can be found at **www.astm.org**.

Received and reviewed under Institute publication policies.

John N. Hardisty is a graduate student at the University of California at Berkeley, Berkeley, CA. He received his BS in civil engineering from Purdue University, West Lafayette, IN.

Enrique Villalobos is a Graduate Engineer at Walter P Moore in Houston, TX. He received his licentiate degree in civil engineering from the University of Costa Rica, San Pedro, Costa Rica, and his MS and PhD in civil engineering from Purdue University.

Brian P. Richter is a Project Engineer at Swenson Say Fagét in Seattle, WA. He received his BS and MS in civil engineering from Purdue University.

Santiago Pujol is an Associate Professor in The School of Civil Engineering at Purdue University. He is a member of ACI Committees 133, Disaster Reconnaissance, and 314, Simplified Design of Concrete Buildings; and Joint ACI-ASCE Committees 441, Reinforced Concrete Columns, and 445, Shear and Torsion.